Collective Excitations in the Charge-Ordered Phase of α-(BEDT-TTF)$_2$I$_3$

T. Ivek,[*] B. Korin-Hamzić, O. Milat, and S. Tomić

Institut za fiziku, P.O. Box 304, HR-10001 Zagreb, Croatia

C. Clauss, N. Drichko, D. Schweitzer, and M. Dressel

Physikalisches Institut, Universität Stuttgart, D-70550, Stuttgart, Germany
(Received 7 December 2009; published 21 May 2010)

The charge response of a charge-ordered state in the organic conductor α-(BEDT-TTF)$_2$I$_3$ is characterized by dc resistivity, dielectric and optical spectroscopy in different crystallographic directions within the two-dimensional conduction layer. Two dielectric modes are detected. The large mode is related to the phasonlike excitation of the $2k_F$ bond-charge density wave which forms in the ab plane. The small dielectric mode is associated with the motion of domain-wall pairs along the a and b axes between two types of domains which are created due to inversion symmetry breaking.

Electron-electron and electron-phonon interactions, in particular, in the systems with reduced dimensionality, are known to be the driving force for the formation of new ordered states of matter [1,2]. Among the most intriguing phenomena found in these systems are broken symmetry phases like charge-density waves (CDW) and spin-density waves, charge order (CO), antiferromagnetic and spin-Peierls phases; all of them show a large variety of nonlinear properties and complex dynamics, including collective excitations [3–6]. This wealth of charge-ordered phenomena in 1D and 2D strongly correlated systems is brought in by the variety in lattice structure, represented by anisotropic networks, both in the electron hopping t and in the intersite Coulomb interaction V. While CO is an effect observed both in inorganic and organic materials with strong electronic correlations, the organics present a more robust and ''clean'' state, where in some cases CO does not compete with other ground states, as opposed to high-temperature superconducting materials, for instance [7].

Theoretical considerations indicate that the charge disproportionation is driven by Coulomb repulsion. In particular, for systems with a quarter filled conduction band even large values of on-site repulsion U are not sufficient to transform the ground state from metallic to insulating; rather, the intersite Coulomb interaction V is responsible to stabilize a Wigner-crystal-type phase (Seo *et al.* in Ref. [8]). Indeed, there are several well-established charge-ordered organic 1D and 2D systems [8]: charge modulation driven by long-range Coulomb repulsion was first evidenced in the 1D organic conductors (DI-DCNQI)$_2$Ag by Kanoda in Ref. [8] and (TMTTF)$_2X$ [9] and also in 2D conductors based on the BEDT-TTF [bis(ethylenedithio)tetrathiafulvalene] molecule: θ-(BEDT-TTF)$_2$RbZn(SCN)$_4$ and α-(BEDT-TTF)$_2$I$_3$ by Takahashi *et al.* [8].

The organic conductor α-(BEDT-TTF)$_2$I$_3$(α-ET$_2$I$_3$) is the most prominent example of charge order in 2D organic

conductors. The crystals are formed by alternating anion and donor layers in the ab plane; the unit cell is triclinic and contains four BEDT-TTF molecules. The BEDT-TTF layer consists of two types of stacks: Stack I is weakly dimerized and composed of crystallographically equivalent molecules A and A', while stack II is a uniform chain composed of B and C molecules [10]. At high temperatures the system is a semimetal with small electron and hole pockets at the Fermi surface [11]. At the metal-to-insulator transition $T_{CO} = 136$ K the conductivity drops by several orders of magnitude and a temperature-dependent gap opens in the charge and spin sector which indicates the insulating and diamagnetic nature of the ground state [10]. Nuclear magnetic resonance (NMR) [12] and synchrotron x-ray diffraction measurements [13] demonstrate that the charge order, whose fluctuations are already observed at high temperatures [14], develops at extended length scales below T_{CO}. The estimated charge values of the molecules are $A = 0.82(9)$, $A' = 0.29(9)$, $B = 0.73(9)$, and $C = 0.26(9)$. The exact site assignment is not settled yet since these values slightly differ from those found in the NMR, vibrational infrared, and Raman spectroscopy [12,15,16]. Observed structural changes comprise two effects. First is a symmetry reduction at the phase transition with the space group $P\bar{1}$ changing into $P1$ in the CO state, which implies four nonequivalent BEDT-TTF molecules in the unit cell. Second is the modulation of overlap integrals due to changes in dihedral angles at low temperatures. In other words, the charge order comprises ''horizontal'' charge stripes along the b crystallographic axis of charge-poor sites, the A' and C molecules, and charge-rich sites, the A and B molecules, together with a bond modulation. The latter infers that the nature of CO in this system should not be regarded as fully localized; instead, a CDW picture would be more suitable.

The considerable knowledge of the CO pattern in α-ET$_2$I$_3$ makes it a suitable candidate in the search for collective excitations in this CO phase. Early results in-

dicated the existence of a broad relaxation in radio-frequency range with a large dielectric constant of the order of 10^5 as well as sample-dependent nonlinearities [17]. In an attempt to characterize the collective excitations of the charge order, we have undertaken dc and ac conductivity-anisotropy measurements on carefully oriented single crystals of α-ET$_2$I$_3$. We discovered a complex and anisotropic dispersion in the charge-ordered state of a 2D organic crystal. First, similar to the Peierls CDW state, we observe long-wavelength charge excitations with an anisotropic phasonlike dispersion, which we detect as broad screened relaxation modes along both the a and b axes of the 2D BEDT-TTF plane. Second, we detect short-wavelength charge excitations in the form of domain-wall pairs, created by breaking the inversion symmetry, which are less mobile and induce a much weaker polarization, again along both crystallographic axes. Also, we observe both types of excitations along diagonal direction of the BEDT-TTF plane. Our results are well understood within the theoretical model by Clay *et al.* [18], which shows that the CO phase with horizontal stripes of localized charges is best described in terms of a bond-charge density wave.

The dc resistivity of α-ET$_2$I$_3$ was measured between room temperature and 40 K. In the frequency range 0.01 Hz–10 MHz the complex dielectric function was obtained from the complex conductance measured by two setups. At high frequencies (40 Hz–10 MHz) an Agilent 4294A precision impedance analyzer was used. At low frequencies (0.01 Hz–3 kHz) a setup for measuring high-impedance samples was used based on lock-in technique. At frequencies 6–10 000 cm^{-1} the complex dielectric function was obtained by a Kramers-Kronig analysis of

the infrared reflectivity. All experiments were done on flat, planar high-quality single crystals along three directions within the plane: in the a and b crystallographic axes as well as in $[1\bar{1}0]$ (diagonal) direction [19]. An influence of extrinsic effects in the dielectric measurements, especially those due to contact resistance and surface layer capacitance, was ruled out with scrutiny [20].

Figure 1(a) shows representative spectra at three selected temperatures for $\mathbf{E} \parallel [1\bar{1}0]$ taken below $T_{CO} = 136.2$ K in the charge-ordered state. Most notably, between 35 K and up to 75 K two dielectric relaxation modes are discerned. The complex dielectric spectra $\varepsilon(\omega)$ can be described by the sum of two generalized Debye functions $\varepsilon(\omega) - \varepsilon_\infty = \Delta\varepsilon_{LD}/[1 + (i\omega\tau_{0,LD})^{1-\alpha_{LD}}] + \Delta\varepsilon_{SD}/[1 + (i\omega\tau_{0,SD})^{1-\alpha_{SD}}]$ where ε_∞ is the high-frequency dielectric constant, $\Delta\varepsilon$ is the dielectric strength, τ_0 the mean relaxation time, and $1 - \alpha$ the symmetric broadening of the relaxation time distribution function of the large (LD) and small (SD) dielectric mode. The broadening parameter $1 - \alpha$ of both modes is typically 0.70 ± 0.05. In Fig. 1(b) the dielectric strengths and mean relaxation times are plotted as a function of inverse temperature. The dielectric strength of both modes does not change significantly with temperature ($\Delta\varepsilon_{LD} \approx 5000$, $\Delta\varepsilon_{SD} \approx 400$). At approximately 75 K the large dielectric mode overlaps the small mode. It is not clear whether the small dielectric mode disappears at this temperature or is merely obscured by the large dielectric mode due to its relative size. However, above 100 K, when the large dielectric mode shifts to high enough frequencies, no indication can be found of a smaller mode centered in the range 10^5–10^6 Hz. Accordingly, above 75 K fits to only one generalized
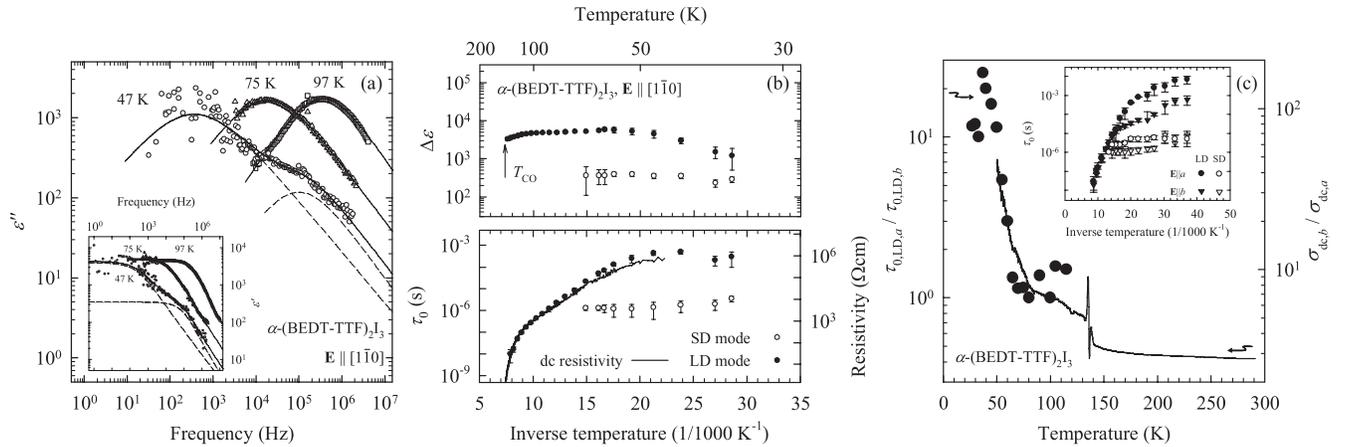

FIG. 1. (a) Frequency dependence of the real (ε') (inset) and imaginary (ε'') part of the dielectric function in α-ET$_2$I$_3$ at representative temperatures for $\mathbf{E} \parallel [1\bar{1}0]$. Below 75 K two relaxation modes are observed—full lines for 47 K show a fit to a sum of two generalized Debye functions, dashed lines represent contributions of the two modes. Above 75 K only one mode is detected, and the full lines represent fits to a single generalized Debye function. (b) Dielectric strength (upper panel) and mean relaxation time with dc resistivity (points and line, respectively, lower panel) in α-ET$_2$I$_3$ as a function of inverse temperature, for $\mathbf{E} \parallel [1\bar{1}0]$. (c) Anisotropy of large dielectric mode mean relaxation times in α-ET$_2$I$_3$ (points, left axis). The temperature behavior closely follows the dc conductivity anisotropy (solid line, right axis). In the inset the mean relaxation time is plotted as a function of inverse temperature: full and empty symbols mark the large and small dielectric mode, respectively, for $\mathbf{E}$ along the a (circles) and b axes (triangles).

Debye function are performed which we identify with the continuation of the large dielectric mode. All three of the large-mode parameters can be extracted in full detail until it exits our frequency window at about 130 K. At temperatures up to 135 K (just below T_{CO}) we can determine only the dielectric relaxation strength by measuring the capacitance at 1 MHz.

The most intriguing result is that the dielectric strength and temperature behavior of the mean relaxation times differ greatly between the two dielectric modes. The large one follows a thermally activated behavior similar to the dc resistivity, whereas the small mode is almost temperature independent. For both orientation $\mathbf{E} \parallel a$ and $\mathbf{E} \parallel b$ the results are comparable to the findings along the $\mathbf{E} \parallel [1\bar{1}0]$. There is no pronounced anisotropy or temperature dependence in the dielectric strength: the $\Delta\varepsilon$ values of both the large and small dielectric modes (not shown) correspond to those measured with $\mathbf{E} \parallel [1\bar{1}0]$. However, an anisotropy in $\tau_{0,LD}$ is clearly visible and its evolution closely follows the dc conductivity anisotropy [Fig. 1(c)]. A similar conductivity anisotropy has been observed in the CO phase of $(TMTTF)_2AsF_6$ [21]. In our samples, despite the temperature-dependent activation, the anisotropic transport gap in the CO phase for $\mathbf{E} \parallel a$ and $\mathbf{E} \parallel b$ can be estimated to about $2\Delta = 80$ and 40 meV. Conversely, our optical measurements for $\mathbf{E} \parallel a$ and $\mathbf{E} \parallel b$ reveal the isotropic gap of about 75 meV [22]. This is not surprising since systems with complex band structure can exhibit distinct optical and transport gaps: optical measurements probe direct transitions between the valence and conduction band, while dc transport is governed by transitions with the smallest energy difference between the two bands.

The observed ac conductivity data demonstrate a complex and anisotropic dispersion in the CO state. First, similar to the CDW state, we observe a broad screened relaxation (large dielectric) mode along the a and b axes and for $\mathbf{E} \parallel [1\bar{1}0]$. This fact indicates that the observed dielectric relaxation is not associated with stripe orientation and its motion along one of the two in-plane crystallographic axes. Rather, this mode can be interpreted as a signature of long-wavelength CDW excitations possessing an anisotropic phasonlike dispersion. A 2D dispersion with similar dielectric strength amplitude and relaxation time behavior was previously found in the commensurate CDW phase developed in ladder layers of $Sr_{14}Cu_{24}O_{41}$ [23–25]. In α-ET$_2$I$_3$ Kakiuchi *et al.* suggested a $2k_F$ CDW formation along the zigzag path CABA'C of large overlap integrals detected in their x-ray diffraction measurements [13]. A theoretical model for the related quarter filled θ-ET$_2$X systems may provide additional insight [18]. Clay *et al.* showed that the CO phase with horizontal stripe phase is characterized by a 1100 modulation of site charges along the two independent p directions parallel to the larger overlap integral, and with a 1010 modulation along the b axis perpendicular to the stripes. In addition, this CO is

accompanied by a modulation of the overlap integrals along the same p direction. In other words, such a CO phase corresponds to the $2k_F$ modulation of bonds and site charges, e.g., a combined bond CDW along the two BEDT-TTF plane p directions. An analogous, albeit more complex, $2k_F$ modulation of overlap integrals indeed develops along the p directions of α-ET$_2$I$_3$, ACA'BA, and ABA'CA (see Fig. 2) [13]. It is plausible to look for the origin of phasonlike dielectric relaxation in such a $2k_F$ bond CDW. In this case the energy scale of barrier heights is close to the single-particle activation energy indicating that screening by single carriers responsible for the dc transport is effective for this relaxation. The fact that the temperature behavior of $\tau_{0,LD}$ anisotropy closely follows the dc conductivity anisotropy has important implications: while the CDW motion is responsible for the dielectric response, the single electron or hole motion along the two p directions, possibly zigzagging between them, is responsible for the observed dc charge transport.

Second, we address the small dielectric mode. Here we note the twinned nature of the CO phase due to breaking the inversion symmetry and formation of a 1010 modulation of site charges along the a axis, with one domain being (A, B) rich and the other (A', B) rich [13]. Indeed, the ferroelectric aspect of the CO phase was also theoretically suggested [8] and experimentally probed [26]. Our data can be naturally attributed to the motion of charged kink-type defects—solitons or domain walls in the CO texture. Charge neutrality constraint of the CO in α-ET$_2$I$_3$ (a change of stripes equivalent to strictly replacing unit cells of one twin type with another) suggests two types of solitons and/or domain walls. The first one is the domain wall in pairs (a soliton-antisoliton pair) between charge-rich and charge-poor stripes along the b axis, which we get if we impose the constraint along the b axis [Fig. 3(a)]. The second type of domain-wall pair is given by applying the constraint along the a axis in such a way that the domain walls' interior contains both charge signs [Fig. 3(b)]. The motion of such entities induces a displacement current and can therefore be considered as the microscopic origin of
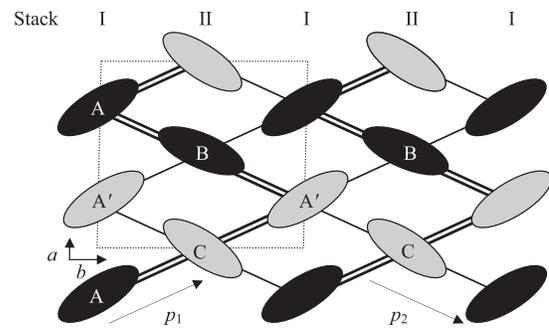

FIG. 2. Schematic representation of a $2k_F$ bond CDW in α-ET$_2$I$_3$. Thin dotted line denotes a unit cell. Single and double lines represent modulated overlap integrals along two p directions (see text).
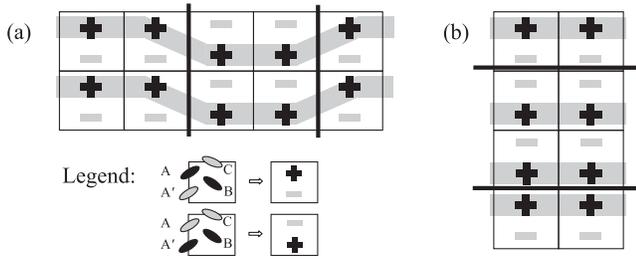
FIG. 3.   Two different types of domain-wall pairs in the charge-ordered phase of α-ET$_2$I$_3$. (A, B)- and (A', B)-rich unit cells are symbolically represented as $+-$ or $-+$ cells which form CO stripes. For simplicity we omit the B and C molecules. Gray thick lines stand for charge-rich stripes. Thin black lines denote a domain-wall pair.

polarization in the CO state. Their relaxation, being nearly temperature independent, cannot be dominated by resistive dissipation, rather it is governed by low-energy barriers, similarly as observed in ferromagnetic domain phase [27]. Finally, the observed dielectric strength $\Delta\varepsilon$ of the small mode of about 400 confirms the domain-wall assignment since their dynamics, in contrast to the phasonlike one, is commonly found to be characterized by much smaller dielectric constants (of the order 1000 and less) [28,29].

In conclusion, we demonstrate the development of in-plane anisotropic conductivity accompanied by the appearance of two low-frequency dielectric relaxation modes in the charge-ordered phase with a horizontal stripe structure of α-(BEDT-TTF)$_2$I$_3$. The large dielectric mode features an anisotropic phasonlike behavior which we associate with the $2k_F$ bond-charge density wave formed within the two p directions in the BEDT-TTF plane. On the other hand, we ascribe the small dielectric mode to the motion of domain-wall pairs at interfaces between two different types of charge order domains created due to inversion symmetry breaking. This unusual appearance of a phasonlike relaxation alongside a solitonlike mode underlines the complexity of collective excitations in such a charge order system. Our results strongly suggest that a localized Wigner-like picture in terms of stripes of localized site charges is not appropriate for charge order in α-(BEDT-TTF)$_2$I$_3$. Instead, our results are consistent with a description in terms of a 2D bond-charge density wave. Our findings demonstrate that the issue of collective excitations in broken symmetry phases becomes ever more subtle and call for further work in order to clarify whether such a dispersion is common to

2D charge order phases with horizontal stripes in diverse strongly correlated systems.

*tivek@ifs.hr; http://real-science.ifs.hr/
[1] P. Fulde, *Electron Correlations in Molecules and Solids* (Springer-Verlag, Berlin, 1995), 3rd ed.
[2] Special issue on Molecular Conductors, edited by P. Batail [Chem. Rev. **104,** 4887 (2004)].
[3] G. Grüner, Rev. Mod. Phys. **60,** 1129 (1988); **66,** 1 (1994).
[4] P. B. Littlewood, Phys. Rev. B **36,** 3108 (1987).
[5] R. J. Cava et al., Phys. Rev. B **31,** 8325 (1985).
[6] T. Vuletić et al., Phys. Rep. **428,** 169 (2006).
[7] J. M. Tranquada et al., Phys. Rev. B **78,** 174529 (2008).
[8] J. Phys. Soc. Jpn. **75,** No. 5 (2006), Special Topics articles 051001–051016.
[9] P. Monceau, F. Y. Nad, and S. Brazovskii, Phys. Rev. Lett. **86,** 4080 (2001).
[10] K. Bender et al., Mol. Cryst. Liq. Cryst. **107,** 45 (1984); **108,** 359 (1984).
[11] T. Mori et al., Chem. Lett. **1984,** 957 (1984).
[12] Y. Takano et al., J. Phys. Chem. Solids **62,** 393 (2001).
[13] T. Kakiuchi et al., J. Phys. Soc. Jpn. **76,** 113702 (2007).
[14] S. Moroto et al., J. Phys. IV (France) **114,** 339 (2004).
[15] J. Moldenhauer et al., Synth. Met. **60,** 31 (1993); M. Dressel and N. Drichko, Chem. Rev. **104,** 5689 (2004).
[16] R. Wojciechowski et al., Phys. Rev. B **67,** 224105 (2003).
[17] M. Dressel et al., J. Phys. I (France) **4,** 579 (1994); M. Dressel et al., Synth. Met. **70,** 929 (1995).
[18] R. T. Clay et al., J. Phys. Soc. Jpn. **71,** 1816 (2002).
[19] Single crystals were oriented in the midinfrared setup before, and in the x-ray setup after experiments.
[20] T. Ivek et al., Phys. Rev. B **78,** 035110 (2008).
[21] B. Korin-Hamzić et al., Phys. Rev. B **73,** 115102 (2006).
[22] C. Clauss, N. Drichko, D. Schweitzer, and M. Dressel, Physica B (Amsterdam) (in press).
[23] T. Vuletić et al., Phys. Rev. Lett. **90,** 257002 (2003).
[24] T. Vuletić et al., Phys. Rev. B **71,** 012508 (2005).
[25] P. Abbamonte et al., Nature (London) **431,** 1078 (2004).
[26] K. Yamamoto et al., J. Phys. Soc. Jpn. **77,** 074709 (2008).
[27] M. Pinterić et al., Eur. Phys. J. B **11,** 217 (1999).
[28] Y. Tokura et al., Phys. Rev. Lett. **63,** 2405 (1989).
[29] S. Tomić et al., Synth. Met. **120,** 695 (2001).